al. 2009). The Japanese 25-year Reanalysis (JRA-25; Onogi et al. 2007) provides surface meteorological variables from 1979 through 2013 to force the land surface model Minimal Advanced Treatments of Surface Interaction and RunOff (MATSIRO; Takata et al. 2003). Realistic month-to-month variability is introduced using the Global Precipitation Climatology Project Version 2.2 (GPCP; Huffman et al. 2012) and Global Precipitation Climatology Centre (GPCC; Rudolf and Rubel 2005) monthly observational precipitation products. Due to the lagged update frequency of the GPCC Full Data Reanalysis Version 6, the Monitoring product Version 4 is used for the period of 2011–13. In order to reconcile the time series of these two separated periods, a trend-preserving statistical bias correction (Watanabe et al. 2012) is applied. In addition, a wind-induced under-catch correction (Legates and Willmott 1990) is applied to GPCC precipitation estimates. Simulated runoff is routed through a global river transfer model, Total Runoff Integrated Pathway (TRIP; Oki and Sud 1998). Simulations are validated over 29 global river basins which encompass approximately 25% (32 358 232 km^2) of the global terrestrial area (130 764 683 km^2). Both flux (discharge) and storage (terrestrial water storage) terms are compared against Global Runoff Data Center in-situ observations and the Gravity Recovery And Climate Experiment (GRACE; Tapley et al. 2004) satellite remote sensing data, respectively (http://hydro.iis.u-tokyo.ac.jp/~hjkim/tws@2009GRL/).

Plates 2.1i and 2.1j show spatial variability of the global river discharge and runoff anomaly in 2013, and Fig. 2.18 shows continent-wise runoff anomaly estimations during the recent four years. Strong spatial variability is apparent during 2013. Within South America, the northwestern part of the continent and most of the Amazon basin show wetter conditions than the climatological mean (1979–2013) in contrast to the drier conditions of the southeastern parts such as Rio de la Plata and Tocantins. In the annual analysis, most of North America suffers from drier conditions than normal, except in the southeastern part of the United States. During the last four years runoff from North America tends to be below the long-term mean, and 2013 is the second driest year following 2012. While the Nile River has more freshwater discharge, the other major river basins on the African continent (e.g., Congo, Niger, Zambezi, and Orange) show less discharge in 2013. The annual discharge from this continent is consistently below the average for the last few years. Relatively weak interannual variability is found in the recent annual estimates of discharge from the European continent. Mediterranean countries are wetter on average while northern European countries are drier leading to a neutral continental balance. The high latitudes of the Eurasia continent and East Asia show negative anomalies particularly for the Yenisei River and its vicinity and rivers in China. The Ob, Amur, and Brahmaputra Rivers transport more water than average. Australia shows extremely large interannual variability. The discharge in 2013 shows a significant negative relative anomaly in contrast to the extreme positive anomaly in 2011.

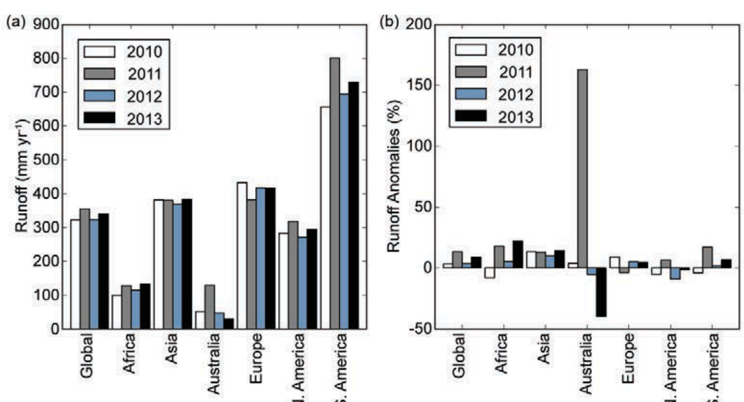

Fig. 2.18. Global and continental estimations for runoff (a) absolute values (mm yr^{-1}) and (b) anomalies relative to the 1979–2013 base period (%) during 2010–13 from the ELSE system.

6) Groundwater and terrestrial water storage—M. Rodell, D. P. Chambers, and J. S. Famiglietti

Terrestrial water storage (TWS) comprises groundwater, soil moisture, surface water, snow, and ice. Groundwater typically varies more slowly than the other TWS components because it is not in direct contact with the atmosphere; however, it often has a larger range of variability on multiannual timescales (Rodell and Famiglietti 2001; Alley et al. 2002). In situ groundwater data are only archived and made available by a few countries. However, monthly TWS variations observed by the Gravity Recovery and Climate Experiment (GRACE; Tapley et al. 2004) satellite mission, which launched in 2002, are a reasonable proxy for unconfined groundwater at climatic scales.

Changes in mean annual TWS from 2012 to 2013 are plotted in Plate 2.1k as equivalent depths of water in cm. TWS can be thought of as an integrator of other hydroclimatic variables (see Plates 2.1d–2.1l). Many parts of the Northern Hemisphere saw a recovery in 2013 from the dry conditions of 2012, while drought continued in other areas. The massive drought that covered most of North America in 2012 abated in much of the eastern and central United States and Canada, but worsened to near-record levels in the southwestern United States. Europe and Russia also recovered from a dry 2012. The year was mixed in southern Asia, with drought afflicting Bangladesh and eastern and southern India. Depletion of aquifers by pumping for irrigation continued in northern India (Rodell et al. 2009; Tiwari et al. 2009) and the North China Plain (Feng et al. 2013), while heavy rains in parts of Turkey and the Middle East helped raise otherwise depressed water levels (Voss et al. 2013). Parts of southern Africa, including Angola and Namibia, went from moderately dry in 2012 to severe drought in 2013. In South America, the central Amazon became extremely wet, while parts of coastal Brazil and Venezuela were dry for most of the year. Australia as a whole lost a large amount of TWS in 2013. Significant reductions in TWS in Greenland, Antarctica, and southern coastal Alaska represent ongoing ice sheet and glacier ablation, not groundwater depletion.

Figures 2.19 and 2.20 show time series of zonal mean and global, deseasonalized monthly TWS anomalies from GRACE, excluding Greenland and Antarctica. Data gaps occur when the satellites were powered down to conserve battery life. Recovery from the unusually dry conditions of 2012 can be seen, particularly in the northern midlatitudes (Fig. 2.19), and also in the global land (Fig. 2.20). The global TWS anomaly ended 2012 at –15 cm, reached an 11-year minimum of –18 cm in February 2013, and recovered to –2 cm by December 2013.

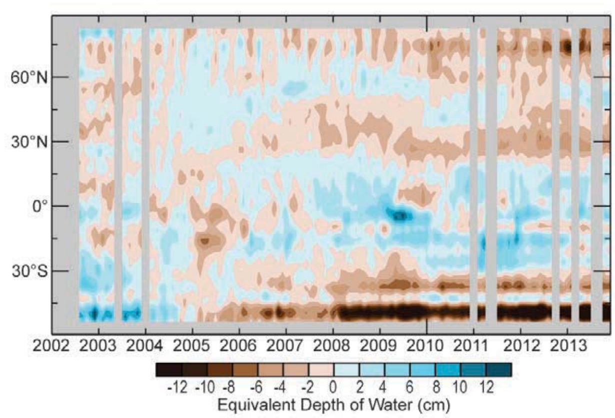

Fig. 2.19. Zonal mean terrestrial water storage anomalies (2003–07 base period) in cm equivalent depth of water, from GRACE. Gray areas indicate months when data were unavailable.

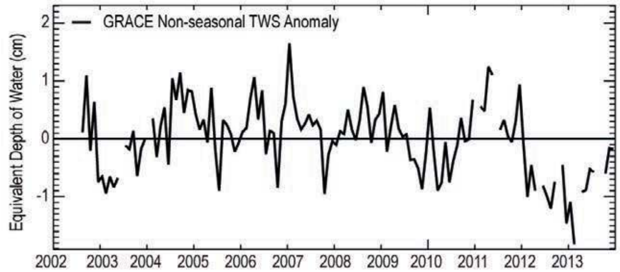

Fig. 2.20. Global average terrestrial water storage anomalies, in cm equivalent depth of water, calculated using a 2003–07 base period. Data gaps occur when the satellites were powered down to conserve battery life.

7) Soil moisture—W. A. Dorigo, D. Chung, R. M. Parinussa, C. Reimer, S. Hahn, Y. Y. Liu, W. Wagner, R. A. M. de Jeu, C. Paulik, and G. Wang

Soil moisture is both a manifestation and a driver of the complex interactions between the water, energy, and biogeochemical cycles at the Earth's surface (e.g., Taylor et al. 2012). Monitoring long-term changes in its mean values and variability is thus pivotal for understanding the effects of climate change (Seneviratne et al. 2010). In 2012 the Climate Change Initiative (CCI) of the European Space Agency released a soil moisture dataset (ECV soil moisture) that amalgamates global observations from various space-borne radiometers and scatterometers (De Jeu et al. 2012a; Liu et al. 2012). Recently, the ECV soil moisture product has undergone several algorithmic improvements and has been complemented with observations from the Coriolis Windsat and GCOM-W AMSR2 sensors to continue the legacy of C-band observations in the passive microwave domain. The observation record now spans a 35-year period (late 1978–present). Anomalies are based on a 1991–2012 climatology. The first 13 years contain different dataset characteristics and so are not included in the climatology.

Plate 2.1l shows where in 2013 either dry (brown) or wet (blue) anomalous conditions prevailed. Anomalous dry conditions were observed in particular in the Southern Hemisphere, e.g., in Argentina, northeastern Brazil, southern Africa, and Australia. These areas are particularly sensitive to drought during the El Niño phase of ENSO (Bauer-Marschallinger et al. 2013; Miralles et al. 2014). However, ENSO conditions were neutral throughout 2013 (see section 2e1). For some of the drought-affected regions (e.g., northeastern Brazil and southern Africa) strong anomalous negative soil moisture conditions were present in 2012 (Parinussa et al. 2013) and continued in 2013. The monthly anomaly maps (Online Fig. S2.15) show that negative anomalies were particularly evident during the first half of 2013, but gradually decreased towards

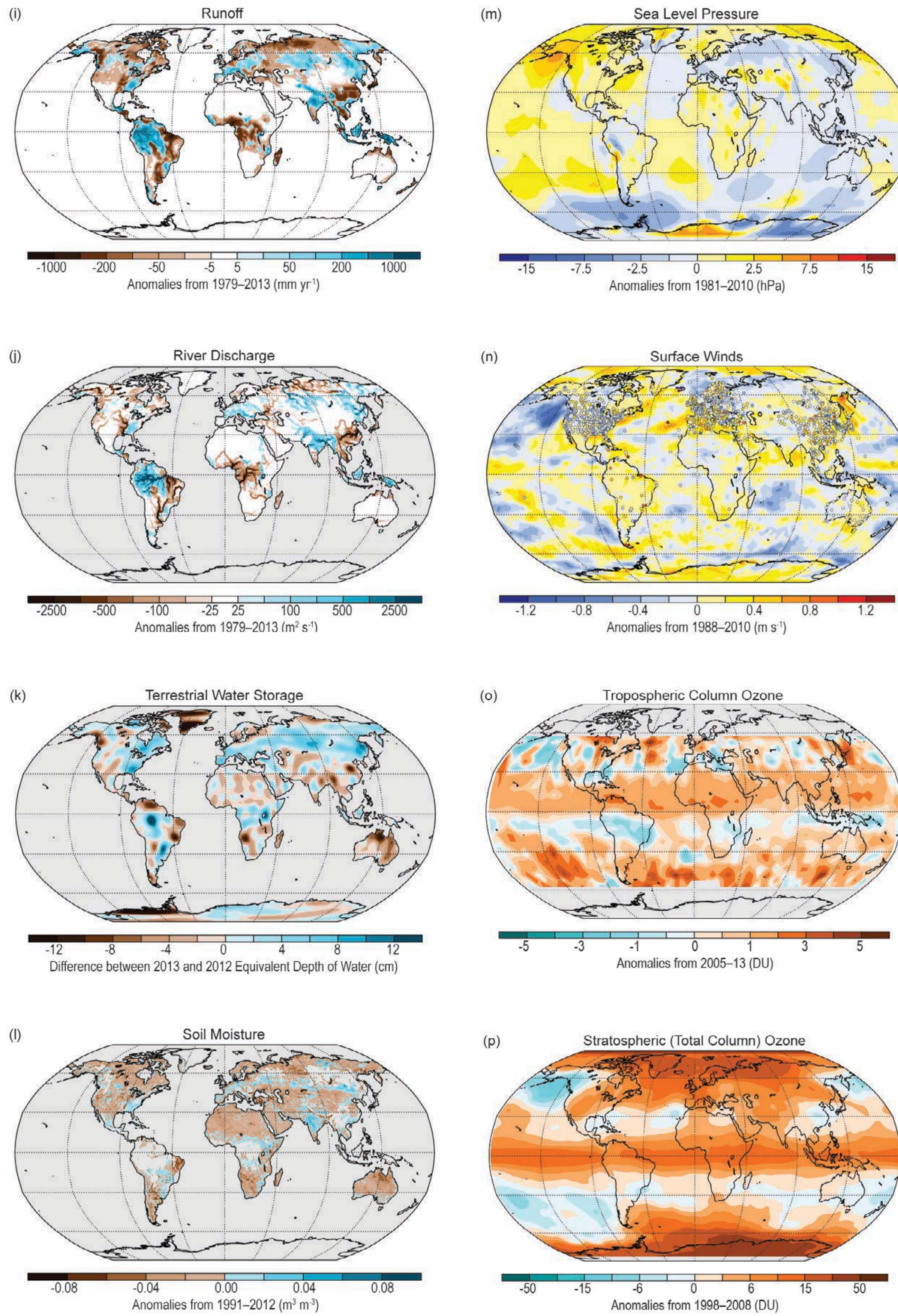
(i)
Runoff
-1000 -200 -50 -5 5 50 200 1000
Anomalies from 1979–2013 (mm yr^{-1})
(m)
Sea Level Pressure
-15 -7.5 -2.5 0 2.5 7.5 15
Anomalies from 1981–2010 (hPa)
(j)
River Discharge
-2500 -500 -100 -25 25 100 500 2500
Anomalies from 1979–2013 (m^2 s^{-1})
(n)
Surface Winds
-1.2 -0.8 -0.4 0 0.4 0.8 1.2
Anomalies from 1988–2010 (m s^{-1})
(k)
Terrestrial Water Storage
-12 -8 -4 0 4 8 12
Difference between 2013 and 2012 Equivalent Depth of Water (cm)
(o)
Tropospheric Column Ozone
-5 -3 -1 0 1 3 5
Anomalies from 2005–13 (DU)
(l)
Soil Moisture
-0.08 -0.04 0.00 0.04 0.08
Anomalies from 1991–2012 (m^3 m^{-3})
(p)
Stratospheric (Total Column) Ozone
-50 -15 -6 0 6 15 50
Anomalies from 1998–2008 (DU)